Neutron-Hole-State Structure in $N = 81$ Nuclei. I. ^{144}Sm and ^{142}Nd (p,d)†

R. K. Jolly and E. Kashy
Cyclotron Laboratory, Michigan State University, East Lansing, Michigan 48823
(Received 7 April 1971)

Angular distributions of deuterons from the (p,d) reaction (energy resolution ~35 keV) on ^{144}Sm and ^{142}Nd at $E_p = 35$ MeV have been measured and compared with distorted-wave Born-approximation (DWBA) calculations. The DWBA calculations were performed both with and without the finite-range and nonlocality corrections. In some typical cases corrections were also included for the nuclear density dependence of the effective pn interaction. The DWBA cross sections for $l = 5$ show an enhanced sensitivity to the inclusion of these corrections. Calculations including both the nonlocality and finite-range corrections yield acceptable spectroscopic factors. Considerable fractionation of the $(2d_{5/2})_\nu^{-1}$ and the $(1g_{7/2})_\nu^{-1}$ states is observed. No measurable population of neutron states in the $82 < N \leq 126$ major shell was observed. The single-neutron-hole energies (in MeV) are as follows: $d_{3/2}$, 0.0; $s_{1/2}$, 0.45; $h_{11/2}$, 1.22; $d_{5/2}$, 1.52; and $g_{7/2}$, 2.12 for ^{143}Sm; and $d_{3/2}$, 0.0; $s_{1/2}$, 0.43; $h_{11/2}$, 1.07; $d_{5/2}$, 1.47; and $g_{7/2}$, 2.20 for ^{141}Nd. Data on the systematics of splitting and movement of these single-neutron-hole states as a function of the proton number (Z) in ^{143}Sm, ^{141}Nd, ^{139}Ce, and ^{137}Ba shall be presented in a subsequent paper.

I. INTRODUCTION

Nuclei with 82 neutrons are expected to have a closed-neutron-shell structure. There is some evidence for this from previous (d, p) measurements[1-3] on targets with 82 neutrons. Another way of checking shell closure at $N = 82$ would be by looking for small occupation probabilities of supposedly vacant shell-model orbits ($2f$ and $3p$ in the present case) via neutron pickup reactions on $N = 82$ nuclei. If shell closure is found to be good in these nuclei, then one may hope that neutron pickup reactions will be a satisfactory means of obtaining information on the neutron-hole states in $N = 81$ nuclei. There have been some (p, d),[4] (d, t)[5,6] and decay-scheme studies[7-9] on isolated cases, but the information obtained is very limited and not backed by enough systematic data to determine reasonably accurate spins and parities and values of single-neutron-hole energies in the $N = 81$ mass region. The present work is the first in a series of measurements to provide such systematic data on the structure of neutron-hole states in $N = 81$ nuclei.

Since the protons are filling some of the same orbits as the neutrons, the present work also provides an opportunity for observing the effect on the binding energy of neutrons owing to the n-p interaction between protons and neutrons in the same shell-model orbits. Furthermore, since the protons in these nuclei do not form a closed or semi-closed shell, they can contribute to some low-lying collective core excitations. Such excitations however do not occur below 1.5 MeV of excitation energy in these nuclei, so that one expects the low-lying states in the $N = 81$ nuclei to be dominantly neutron-hole states. States at higher excitation energies however, may be expected to have appreciable core excitation components mixed in them, resulting in splitting of the single-neutron-hole states.

The following section describes the experimental arrangement used in the present work. Section III describes details of three types of distorted-wave Born-approximation (DWBA) calculations performed to determine the effect of various corrections on the shape and the magnitude of the predicted differential cross sections. In Sec. IV we present the experimental results, the computed values of single-hole energies and strengths, etc., followed by a discussion of these results.

II. EXPERIMENTAL PROCEDURE

35-MeV protons from the Michigan State University variable energy cyclotron bombarded targets of ^{144}Sm and ^{142}Nd and the reaction products were analyzed in a cooled and radiation shielded ΔE-E counter telescope. The counter telescope was also equipped with magnets for electron suppression so that with a combination of the aforesaid features and a proper choice of amplifier time constants, an over-all energy resolution of ~35 keV was achieved. Particle selection was accomplished by displaying ΔE vs E in a two-parameter analysis mode where the reaction products were sorted out by drawing polynomial fits around their respective curved bands using a data acquisition program TOOTSIE.[10]

The targets (see Table I for target data and (p, d) ground-state Q values[11]) were prepared in the cyclotron laboratory by evaporating isotopically enriched inorganic compounds from a graphite boat

TABLE I. ^{144}Sm and ^{142}Nd target data and $(p, d)Q$ values.

Isotopic target	Chemical form	Enrichment (%)	$Q(p, d)$[a] (MeV)
^{144}Sm	Sm_2O_3	95.1	-8.24 ± 0.08
^{142}Nd	Nd_2O_3	97.6	-7.584 ± 0.024

[a] See Ref. 11.

heated by electron bombardment. To prevent subsequent damage to targets (on account of their tendency to form flakes), the evaporated films were sandwiched between single layers (~5 μg/cm^2) of Formvar.

To detect any unresolved multiplets in the low-lying states of the energy spectra in the present work, high-resolution (10–14 keV) measurements were also made with a pair of thin cooled position-sensitive detectors[12] in the focal plane of our Enge split-pole spectrometer.

Absolute cross sections were obtained by simultaneously measuring (p, p) and (p, d) spectra at 30, 40, and 50° and fitting these limited elastic scattering angular distributions to the optical-model predictions using the same parameters as in the DWBA calculations described below. The uncertainty in this normalization procedure is estimated at $\lesssim 10\%$.

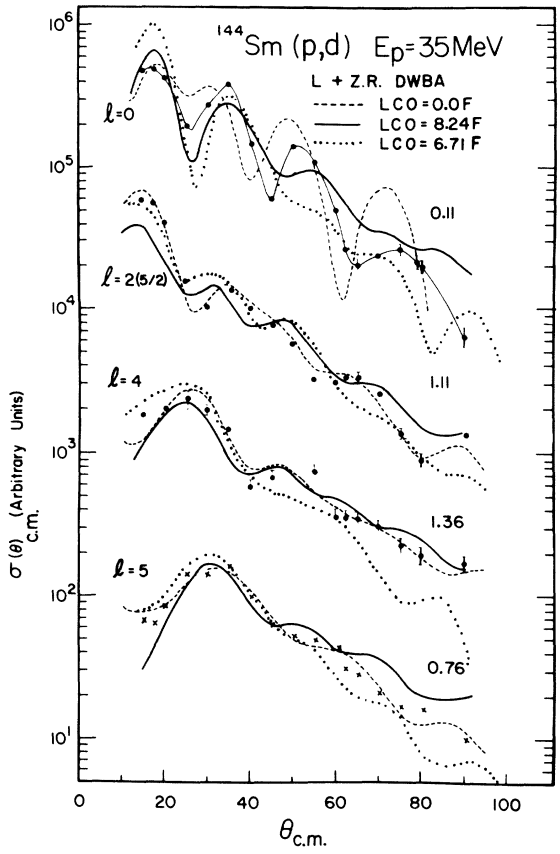

FIG. 1. A comparison of local and zero-range DWBA calculations, with different values of the lower cutoff radius, with the experimental angular distributions for the strongest deuteron groups in ^{144}Sm(p, d).

TABLE II. Optical-model parameters for protons (derived from Ref. 14) and deuterons (derived from Ref. 16) used in the present calculations. The symbols used have their usual meaning (see Refs. 14 and 16). All lengths are in fermis and all depths are in MeV.

Protons (E = 35 MeV) Nuclide	V_s	W_d	V_{so}	Deuterons (E ~ 25 MeV) Nuclide	V_s	W_d
^{144}Sm	42.6	12.0	8.5	^{143}Sm	97.0	17.3
^{142}Nd	42.8	12.9	8.5	^{141}Nd	97.5	17.0
Fixed geom. $r_{0I}=r_{0S}=r_C=1.25$				Fixed geom. $r_{0S}=r_{0C}=1.15$		
Parameters $a_s=0.65$, $a_I=0.47$.				Parameters $a_s=0.81$, $a_I=0.68$, $r_{0I}=1.34$		
Nonlocality parameter $\beta=0.85$ F				Nonlocality parameter $\beta=0.54$ F		

III. DWBA CALCULATIONS

To extract spectroscopic information from the experimental data, DWBA calculations were performed using the Oak Ridge National Laboratory (ORNL) code JULIE.[13] The fixed-geometry optical-model parameters of Perey[14] extrapolated to proton energies of 35 MeV were used. Although the parameters of Fricke *et al.*[15] are perhaps more appropriate at this energy, the analysis of Fricke *et al.* lacks any systematics on the variation of the imaginary well depth with energy and mass number, so that these parameters will have to be guessed for the nuclei studied in the present work. The deuteron parameters used were derived from the work of Perey and Perey.[16] Once again these were fixed-geometry average parameters and also did not include any spin-orbit interaction. Both the proton and the deuteron parameters are listed in Table II. The calculations were performed for neutrons being picked up from the $2d_{3/2}$, $3s_{1/2}$, $1h_{11/2}$, $2d_{5/2}$, and $1g_{7/2}$ orbits.

Initial calculations were performed in the local and zero-range (henceforth referred to as LZR calculations) DWBA. Several values of the lower cutoff near the surface were tried. The results of these calculations are compared in Fig. 1 with the strongest $l=0$, $2(\frac{5}{2})^+$, 4, and 5 transitions in ^{144}Sm-$(p, d)^{143}$Sm reaction. In the case of the $l=0$ transition, none of the calculations reproduce the shape of the experimental angular distribution very well although the calculations with nonzero values of the lower cutoff do predict the locations of the first few maxima and minima correctly. For the other l values, the data definitely favor calcula-

tions without a lower cutoff.

These calculations were repeated including the corrections due to the nonlocality of the deuteron and proton optical potentials and the finite range of the effective p-n interaction that appears in the (p,d) transition matrix element.[13] These calculations shall be henceforth referred to as NLFR calculations. Values of the nonlocality parameter were taken to be 0.85 F for protons[17] and 0.54 F for deuterons.[18] (The potential for the bound-state wave function was taken to be local since it is not certain as to how one treats the nonlocality in the bound-state wave function correctly.) Both of these corrections suppress the (p,d) form factor[13] in the nuclear interior and thus accomplish the same result as a lower cutoff does. The results can be seen in Fig. 2 where the experimental angular distributions have compared with LZR and NLFR-DWBA calculations arbitrarily normalized to the experimental cross sections. A third type of calculation also shown in Fig. 2 includes in addition the effect of the nuclear matter density dependence of the effective p-n interaction (e.g., see Green[19]). These calculations shall be henceforth called NLFR + DD calculations. It has been demonstrated that these density-dependent effects are significant in bringing about an agreement between DWBA calculations and the experimental cross sections in lighter nuclei[20] like ^{16}O. The study of these effects in the heavy nuclei investigated here is, therefore, of some interest. In the density-dependent calculations the radial form factor was modified by

$$F(r) = [1 - 1.845\rho^{2/3}(r)],$$

where

$$\rho(r) = 0.17(1 + e^{X})^{-1}, \quad X = (r - r_0 A^{1/3})/a. \qquad (1)$$

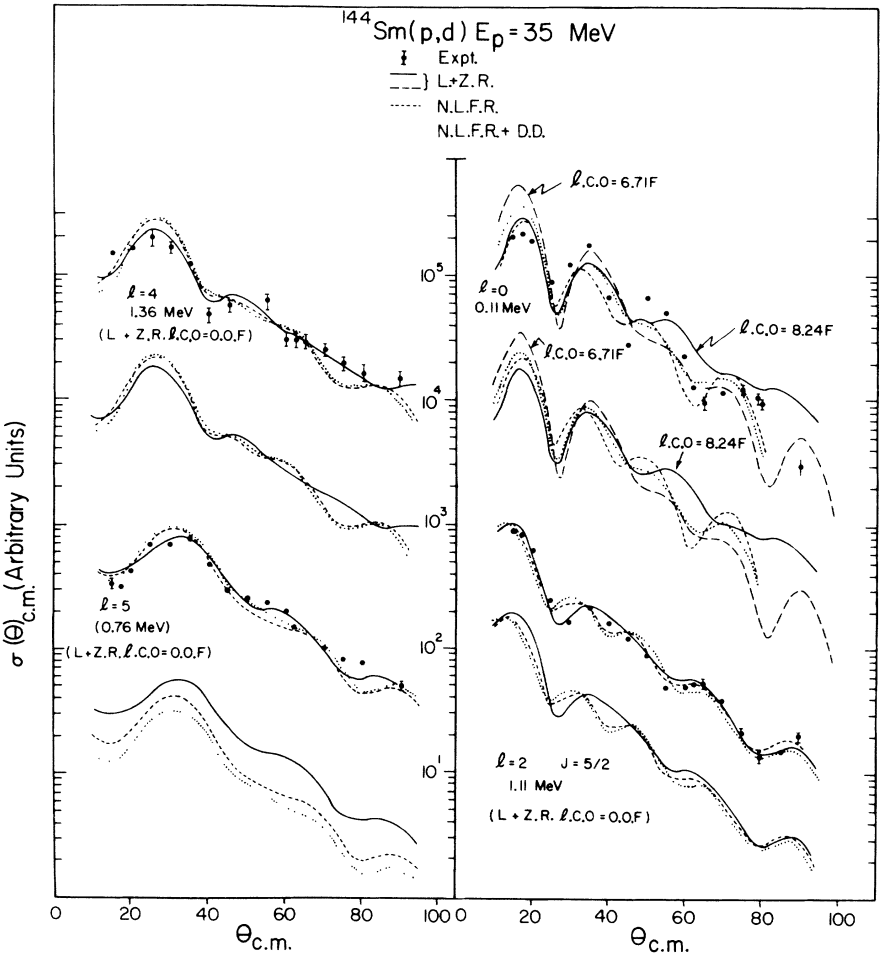

FIG. 2. A comparison of the local and zero range (L + ZR), nonlocal and finite range (NLFR), and NLFR with correction for nuclear density dependence of the p-n interaction (NLFR + DD) DWBA calculations with the experimental angular distributions for the strongest groups in ^{144}Sm(p,d). The various calculations have also been compared among themselves (and without the experimental angular distributions) to indicate their effect on the spectroscopic factors.

Such a factor has been suggested in Ref. 19. An examination of Fig. 2 shows the differences in the shapes (compared with those of the experimental angular distributions) and magnitudes of the differential cross sections predicted by the various calculations mentioned above. The magnitudes of the DWBA cross sections have been compared only among the different calculations and not with the experimental data. In the case of $l=0$, the LZR DWBA calculation is with a lower cutoff of 8.24 F. With the exception of $l=5$ where one observes changes in the calculated cross sections by a factor of 2, the predicted cross sections for the various calculations are similar to within 30% for $l=0$, 2, and 4. The shapes of the various DWBA angular distributions are also very similar in gross features although in detail the NLFR and NLFR +DD calculations tend to be slightly more oscillatory than the LZR calculations (probably on account of the increased l-space localization due to some damping of the form factor in the nuclear interior in the former cases). It is not certain if the density-dependent damping used in the present calculations is a correct one to use. This coupled with the fact that such a damping does not affect the shapes or the magnitudes (except for $l=5$, where the effect on magnitude is larger than in other cases) of the calculated cross sections appreciably, persuaded the authors to adhere to the NLFR calculations for analysis of the experimental cross sections for spectroscopic information. Consequently all DWBA calculations shall, henceforth, be only of the NLFR variety.

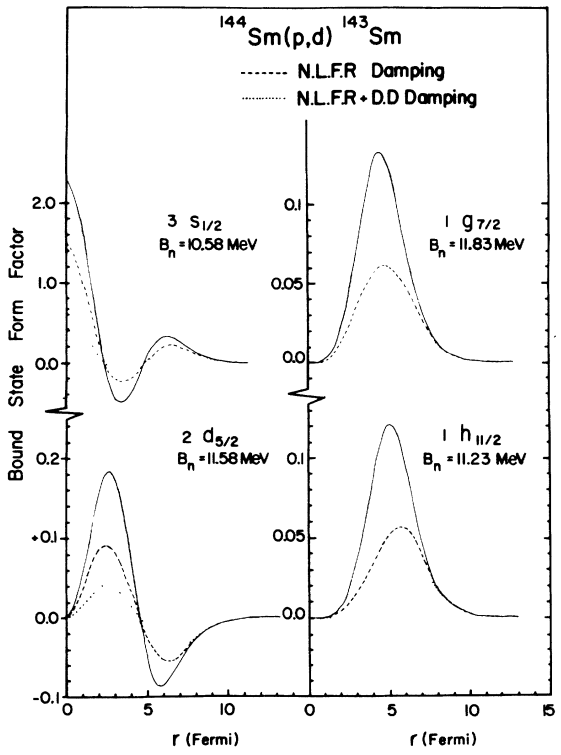

FIG. 3. Damping of the local- and zero-range- (p,d) form factors (solid curves) caused by the inclusion of nonlocality, finite-range, and density-dependent corrections. B_N are binding energies of the transferred nucleon for the shell-model orbits shown in the figure.

In Fig. 3 we show the extent of damping of the (p,d) form factor in the nuclear interior caused by the inclusion of nonlocality and finite range corrections (the broken curves) and also the density-dependent correction (the dotted curves). A comparative examination of Figs. 2 and 3 shows that the magnitudes of the various DWBA cross sections for $l=5$ in Fig. 2 show enhanced sensitivity to the inclusion of the aforesaid corrections because in the case of the smaller l values the contribution to the DWBA cross section from the nuclear interior (where the smaller-l-value form factors tend to peak) is greatly suppressed by the strong absorption (specially for deuterons) of the distorted waves.

The NLFR calculations described above were used to extract spectroscopic factors by fitting the experimental angular distributions to the DWBA cross sections. The two are related by[13]

$$\sigma_{\text{expt}}(\theta) = \tfrac{3}{2} D_0^2 S \sigma_{\text{DWBA}}(\theta) . \tag{2}$$

There is no arbitrary normalization in this equality. The value of the overlap integral D_0^2 is taken to be 1.6 using the Hulthen wave function for the deuteron and including the contribution from the D state of the deuteron.[21] Since the (p,d) reaction can populate both the $T_>$ and the $T_<$ states in the final nucleus, the total spectroscopic strength for a given orbital Nlj will be divided among these states. Only $T_<$ states were observed in the present measurements so that the sum rule for the spectroscopic factors measured here is given by[22]

$$S_<^{Nlj} = \nu^{Nlj} - \pi^{Nlj}/(2T+1) , \tag{3}$$

where ν^{Nlj} and π^{Nlj} are the numbers of neutrons and protons occupying the shell-model orbitals Nlj. Centroid energies for the various single-hole states were calculated as average energies weighted by the spectroscopic factors S_i of the various components of the single-neutron-hole states, i.e.,

$$\bar{E}_{Nlj} = \frac{(\sum_i S_i E_i)_{Nlj}}{(\sum_i S_i)_{Nlj}} . \tag{4}$$

Values of the single-neutron-hole energies and strengths in the nuclei of ^{143}Sm and ^{141}Nd obtained in the present work shall be presented in the following section.

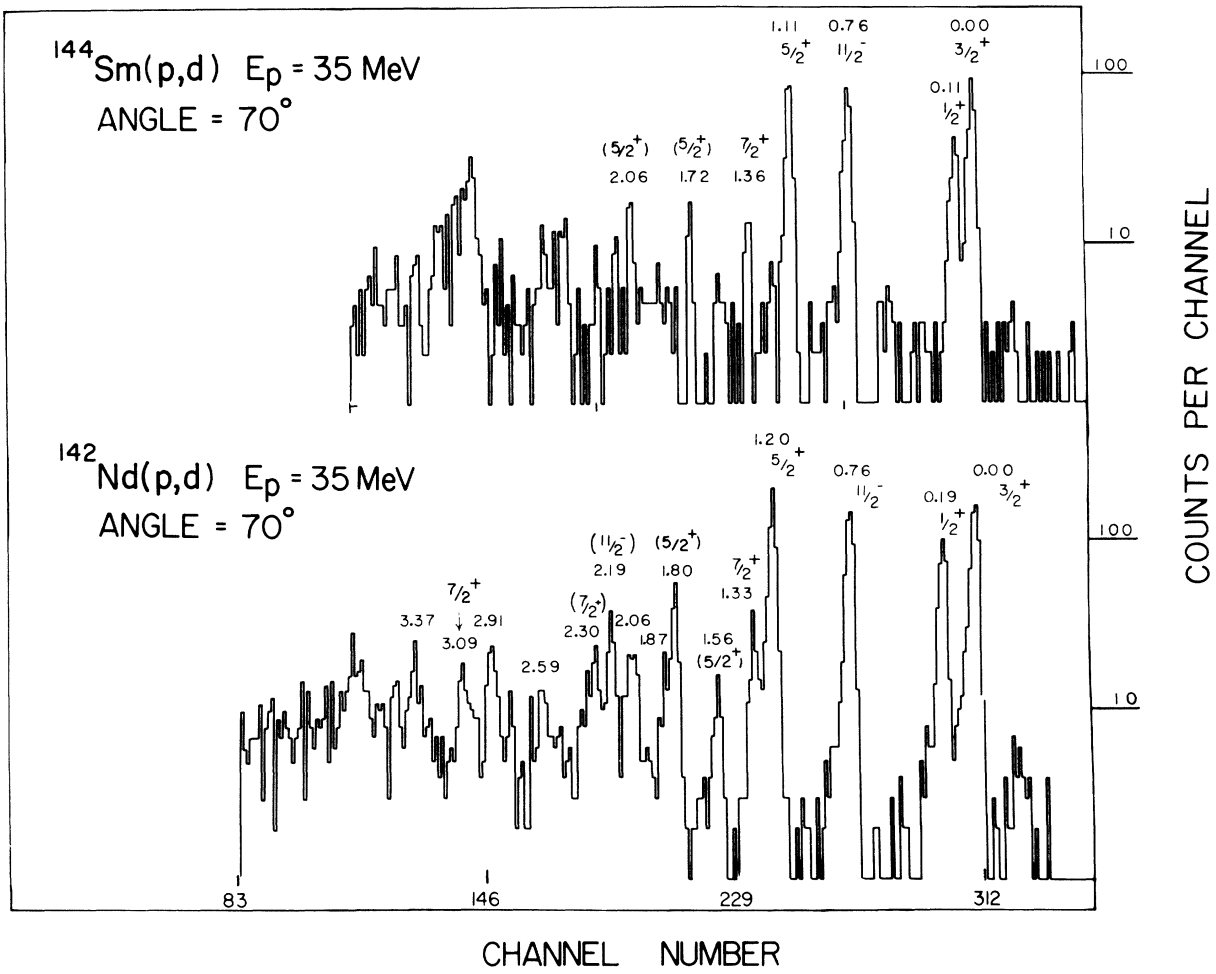

FIG. 4. Sample (p,d) energy spectra from ^{144}Sm and ^{142}Nd at $E_p = 35$ MeV.

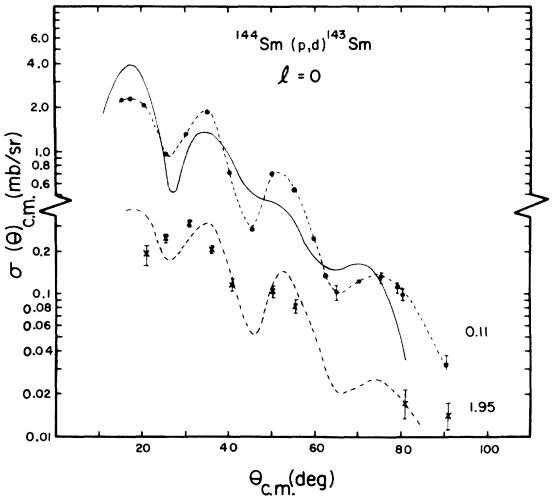

FIG. 5. A comparison of the experimental angular distributions for the 0.11- and the 1.95-MeV states in ^{143}Sm with the NLFR-DWBA calculation for $l = 0$. The broken curves are empirical.

IV. RESULTS AND DISCUSSION

A. ^{144}Sm(p,d)

A sample energy spectrum from this reaction is shown in the top part of Fig. 4. An obvious feature of the spectrum is the strongly excited low-lying states, the first four of which are the dominant components of the $2d_{3/2}$, $3s_{1/2}$, $1h_{11/2}$, and $2d_{5/2}$ neutron-hole states.

Angular distributions of these and several other states were measured from 15 to 90°. These are shown in Figs. 5, 6, 8, and 9 where the data have been compared with NLFR-DWBA calculations shown as broken and solid curves (exception: 0.11-MeV state in Fig. 5, where the broken curve is drawn through the data points only to guide the eye). The agreement between the angular distributions of the strongly excited states and the DWBA calculations is generally good with the exception of the 0.11-MeV state ($l=0$, Fig. 5), where the locations of the maxima and minima and the general trend

of the differential cross sections are reproduced but the agreement between theory and experiment is far from perfect.

Several $l=2$ angular distributions are shown in Fig. 6. The ground state of ^{143}Sm is known to be $\frac{3}{2}^+$ and it agrees with the $l=2$, $J=\frac{3}{2}$ calculation reasonably well. The first excited state with an $l=2$ angular distribution is at 1.11 MeV of excitation energy in ^{143}Sm. It is as strongly excited as the ground state and is assigned $J=\frac{5}{2}$ on the basis of sum-rule arguments. The almost identical angular distributions of the $d_{3/2}$ ground states of ^{143}Sm and ^{141}Nd have been combined and compared with the similarly combined angular distributions of the first excited $l=2$ ($J=\frac{5}{2}$) states to look for any J-dependent effects in these angular distributions.

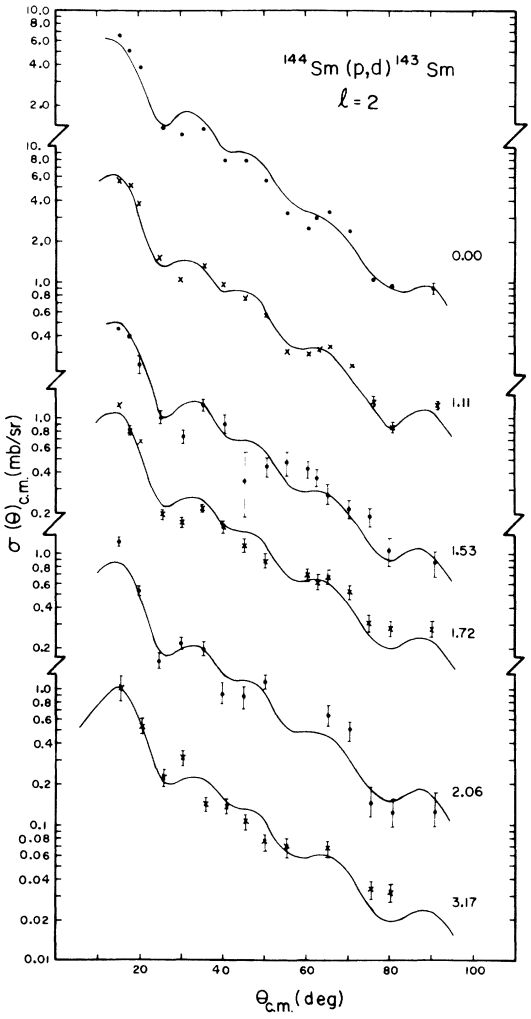

FIG. 6. A comparison of the experimental angular distributions for several states in ^{143}Sm (excitation energies on the right-hand side) with the NLFR-DWBA calculations for $l=2$. With the exception of the ground state, all others were assumed to have a spin and parity of $\frac{5}{2}^+$.

A similar procedure was followed for the nuclei of ^{139}Ce and ^{137}Ba. The results are shown in Fig. 7. It is apparent that there are no significant J-dependent effects that could be relied upon for spin assignments. The dip in the $\frac{3}{2}^+$ angular distribution in the upper part of Fig. 7 is real as it occurs in the data for both Sm and Nd, but does not occur in the case of Ba and Ce.

At least four possible $l=4$ angular distributions are observed for the states at 1.36, 2.16, 2.29, and 3.04 MeV of excitation energy (Fig. 8). Although the error bars in these data are large, the angular distributions do not resemble the $l=5$ DWBA calculations. None of these angular distributions even remotely resemble the angular distribution for an $l=3$ transfer. As we shall see in the following pages, no transition with an angular distribution similar to an $l=3$ calculation was observed with any measurable intensity in the entire present work, thus pointing to the good neutron shell closure in these $N=82$ nuclei.

In Fig. 9 at least two states at 0.76 and 2.47 MeV of excitation energy have angular distributions that

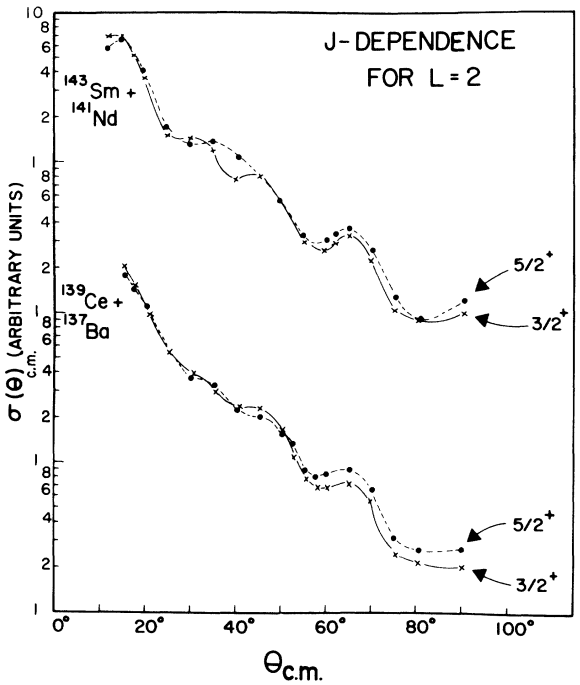

FIG. 7. Comparison of the ground state $d_{3/2}$ and the first excited (and also the strongest) $d_{5/2}$ state angular distributions to indicate any possible J-dependent effects. The $d_{3/2}(d_{5/2})$ angular distributions for both ^{143}Sm and ^{141}Nd are very similar and, therefore, were combined to average out fluctuations that might mask any systematic J-dependent effects. The dip in the 40° point for the $d_{3/2}$ angular distribution was observed in the data for both ^{143}Sm and ^{141}Nd. The data for ^{139}Ce and ^{137}Ba are taken from Ref. 23.

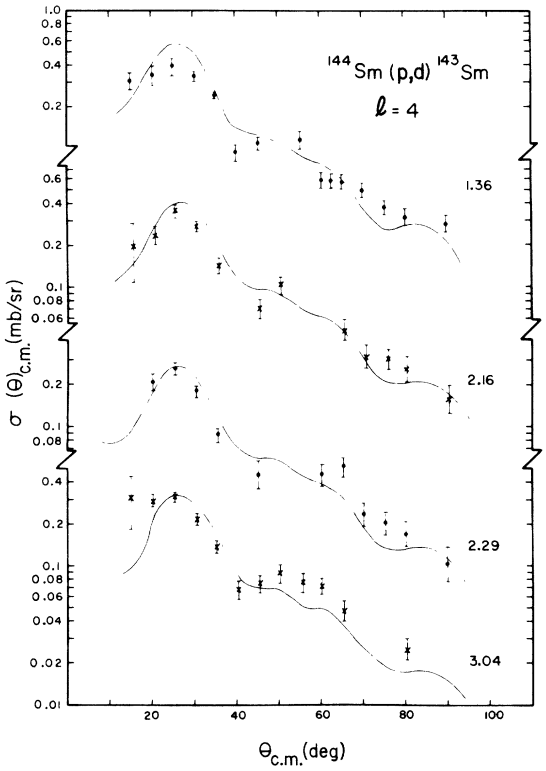

FIG. 8. A comparison of the experimental angular distributions for several states in ^{143}Sm (excitation energies shown on the right-hand side) with NLFR-DWBA calculations for $l=4$.

agree well with $l=5$ DWBA calculations. These assignments are further supported by the existence of two $l=5$ states at similar excitation energies in the other $N=81$ nuclei investigated in the present sequence. The $l=5$ assignment for the 2.59-MeV state is not as certain because of the relatively large scatter of the experimental points.

The excitation energies of the various states in ^{143}Sm observed in the present work along with their spins and parities (wherever assigned), absolute spectroscopic factors obtained by using Eq. (2), together with relative spectroscopic factors (based on the assumption that the spectroscopic factor for the $d_{3/2}$ ground state is 4.0) are listed in Table III. The only ambiguity in J^π assignment occurs in the case of $l=2$ transitions for the excited states of ^{143}Sm. As pointed out earlier, J-dependent effects (if any) for $l=2$ are too small to enable us to distinguish between $J=\frac{5}{2}$ and $J=\frac{3}{2}$. However, other arguments listed below, tend to suggest that probably all the strongly excited higher-lying $l=2$ states are of $J^\pi=\frac{5}{2}^+$. This is because:

(i) In all nuclei studied in the $N=82$ (p,d) program, there is an energy gap of $\gtrsim$1.5 MeV between the ground state and the first $l=2$ excited state.

(ii) The ground state practically exhausts all of the $(d_{3/2})_\nu^{-1}$ strength in these nuclei. Assuming all the higher $l=2$ transitions to be $\frac{5}{2}^+$ yields consistent values of the total $(d_{5/2})_\nu^{-1}$ strength and centroid energies in all $N=82$ nuclei investigated in

TABLE III. Excitation energies, l and J^π assignments, (p,d) cross sections at the observation angle θ, absolute and relative spectroscopic factors for the various states observed in the ^{144}Sm$(p,d)^{143}$Sm reactions.

Excitation energy (MeV)	l	J^π	$\theta_{c.m.}$ (deg.)	$\sigma(\theta)_{c.m.}$ (mb/sr)	S	S (relative)
0.00	2	$\frac{3}{2}^+$	25.3	1.42	3.3	4.0
0.11	0	$\frac{1}{2}^+$	20.2	2.10	1.1	1.4
0.76	5	$\frac{11}{2}^-$	35.4	1.80	6.1	7.4
1.11	2	$\frac{5}{2}^+$	35.4	1.32	3.0	3.7
1.36	4	$\frac{7}{2}^+$	35.4	0.25	2.5	3.1
1.53	2	$\frac{5}{2}^+$	35.4	0.13	0.28	0.34
1.72	2	$\frac{5}{2}^+$	20.2	0.68	0.6	0.8
(1.95)	(0)	$(\frac{1}{2}^+)$	40.4	0.12	0.2	0.3
2.06	2	$\frac{5}{2}^+$	20.2	0.53	0.5	0.6
2.16	4	$\frac{7}{2}^+$	50.5	0.10	2.2	2.7
2.29	4	$\frac{7}{2}^+$	20.2	0.21	1.5	1.8
2.47	5	$\frac{11}{2}^+$	35.4	0.30	1.1	1.4
2.59	(5)	$(\frac{11}{2}^-)$	35.4	0.18	0.66	0.84
3.04	(4)	$(\frac{7}{2}^+)$	45.5	0.07	1.9	2.1
3.17	(2)	$(\frac{5}{2}^+)$	25.3	0.23	0.6	0.7

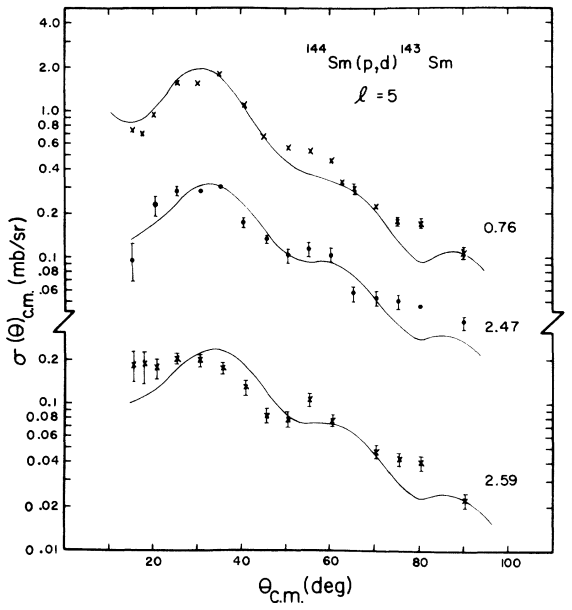

FIG. 9. A comparison of experimental angular distributions for three states in ^{143}Sm (excitation energies shown on the right-hand side) with NLFR-DWBA calculations for $l=5$.

the present sequence.

(iii) The shell-model order of the $2d_{3/2}$ and $2d_{5/2}$ states adopted here (i.e., $d_{5/2}$ lies deeper in $N=82$ nuclei) is consistent with the $(d, {}^3\mathrm{He})^{23}$ and $(t, \alpha)^{24}$ studies made on ^{208}Pb.

(iv) Assuming that all the high-lying $l=2$ states are of spin and parity $\frac{5}{2}^+$, it is apparent that the $(d_{5/2})_\nu^{-1}$ state is split into at least five components. A systematic variation of the spectroscopic factors and energies of these components as one goes through the spectra of the various odd-A, $N=81$ nuclei is observed[25] so that assigning a $J^\pi=\frac{3}{2}^+$ even to one of the weaker (e.g., one at 1.53 MeV) $l=2$ transitions would imply too large a strength for the $(d_{3/2})_\nu^{-1}$ state and too small a strength for the $(d_{5/2})_\nu^{-1}$ state in ^{137}Ba.

Hence on the basis of these arguments tentative spin and parity assignments of $\frac{5}{2}^+$ have been made to all the excited $l=2$ states.

The energy levels of ^{143}Sm along with their J^π assignments and spectroscopic factors are shown in Fig. 10 where these have been compared with the preliminary results of Bruge *et al.*[26] and the unpublished results of Edwards *et al.*[27] Our energy levels essentially agree with those of Refs. 26

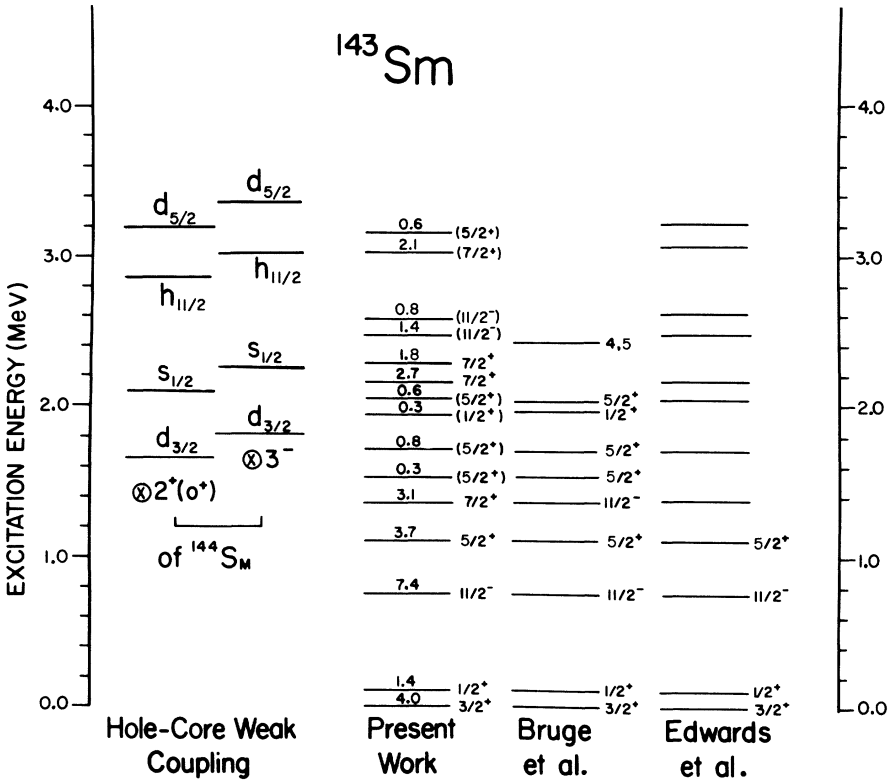

FIG. 10. A comparison of the present results in ^{144}Sm$(p,d)^{143}$Sm with the preliminary (unpublished) results of Bruge *et al.* (Ref. 26) and Edwards *et al.* (Ref. 27). The numbers above the energy levels in the present work are relative spectroscopic factors. A comparison is also made between the neutron-hole states weakly coupled to the 2^+ and the 3^- core excitations of ^{144}Sm and the ^{143}Sm energy levels. See text for further comments.

TABLE IV. Sums of spectroscopic strengths and centroids of single-neutron-hole energies.

^{143}Sm Nlj	$(\sum_i S_i)_{Nlj}$ Absolute	$(\sum_i S_i)_{Nlj}$ Relative	Theoretical	$\frac{(\bar{E}_{Nlj}-\bar{E}_{2d_{3/2}})}{=\frac{(\sum_i S_i E_i)_{Nlj}}{(\sum_i S_i)_{Nlj}}}$ (MeV)
$2d_{3/2}$	3.3	4.0	4.0	0.0
$3S_{1/2}$	1.42	1.7	2.0	0.45
$1h_{11/2}$	7.9	9.6	12.0	1.22
$2d_{5/2}$	5.0	6.0	5.0	1.52
$1g_{7/2}$	8.1	9.8	7.9	2.12
^{141}Nd				
$2d_{3/2}$	4.1	4.00	4.0	0.00
$3S_{1/2}$	2.3	2.3	2.0	0.43
$1h_{11/2}$	11.4	11.1	12.0	1.07
$2d_{5/2}$	5.9	5.7	5.9	1.47
$1g_{7/2}$	10.5	10.2	7.9	2.20

and 27 whenever the same levels have been measured in all three experiments. The spin and parity assignments also largely agree, with the exception of the 1.36-MeV state. Our angular distribution (Fig. 8) agrees with the DWBA calculation for $l=4$ and does not agree with $l=5$. Furthermore the energy systematics of the various components of $(1h_{11/2})_\nu^{-1}$ and $(1g_{7/2})_\nu^{-1}$ states[25] favor our assignment. In the case of the 2.47-MeV state our angular distribution definitely favors an $l=5$ assignment (Fig. 9). For the case of the 2.59-MeV state our angular distribution somewhat favors an $l=5$ over an $l=4$. The uncertainty in the data for the latter state is partly due to a high local density of states at this excitation energy, so that it is conceivable that this state may be a multiplet. However, observation of the line shape of this state as a function of angle does not seem to support the multiplet structure hypothesis for this state unless all the members of the multiplet are almost degenerate and have similar angular distributions.

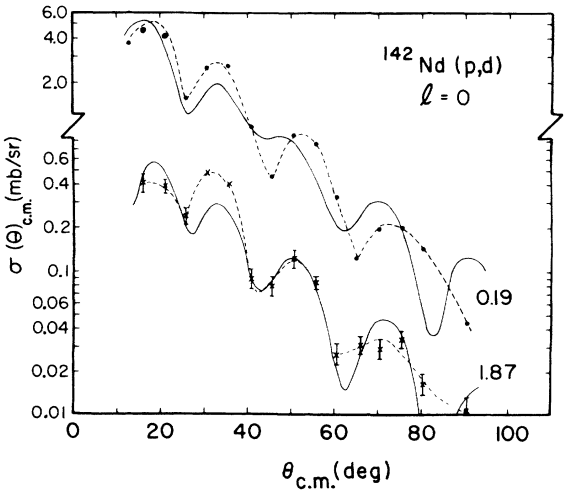

FIG. 11. A comparison of the experimental angular distributions for the 0.19- and the 1.87-MeV states in ^{141}Nd with the NLFR-DWBA calculation for $l=0$. The broken curves are empirical.

In the case of the 1.95-MeV state, Bruge *et al.*[26] claim a spin and parity assignment of $\frac{1}{2}^+$. Our angular distribution data are sparse (Fig. 5) but not inconsistent with an $l=0$ angular distribution. This is further supported by the energy systematics of the two components of the $(s_{1/2})_\nu^{-1}$ neutron state observed in other odd-A $N=81$ nuclei.

Values of the single-neutron-hole energies for the various shell-model orbits in the $50<N\leq 82$ range were calculated relative to $E_{2d_{3/2}}$ and are listed in Table IV along with the summed hole strengths for these states. Both the absolute and the relative values (obtained by assuming $S_{d_{3/2}}=4.0$) of these strengths are listed and compared with theoretical values calculated from Eq. (3). Comparing the relative spectroscopic factors with the theoretical values, it appears that some of the $1h_{11/2}$ strength has been missed while in the case of $1g_{7/2}$ we have an excess of strength. Here one might suspect a case of wrong l-value assignments. However the cross sections (both experimental and DWBA) for $l=4$ are so much smaller than those for $l=5$, that we will have to assign all $l=4$ transitions to $l=5$ to make up for the missing strength. Obviously that is not the answer. Perhaps the explanation lies in the sensitivity of the $l=5$ DWBA calculations to the extent of internal damping caused by the various corrections as we saw in Figs. 2 and 3. The overestimate in the case of $l=4$ is probably due to the large experimental uncertainties in the small cross sections for $(1g_{7/2})_\nu^{-1}$ states. In the cases of ^{137}Ba and ^{139}Ce the $(1g_{7/2})_\nu^{-1}$ strengths are slightly underestimated.[25]

The single-neutron-hole energies have been added, respectively, to the energies of the lowest 2^+ and 3^- core excited states of ^{144}Sm to get the locations

of the centers of gravity of these core excitations weakly coupled to the various single-neutron-hole states. Of course, only such core-hole coupled states as have a nonnegligible hole-state component in the complete-state wave function will be observed with measurable cross sections in (p,d) measurements. An examination of Fig. 10 indicates that probably the 1.53- and 1.73-MeV d ($l=2$) states have an appreciable $(d_{3/2})_\nu^{-1}\otimes 2^+$ component. Similar comments may also be made about the $(d_{5/2})_\nu^{-1}\otimes 2^+$ component in the 3.17-MeV $l=2$ state and the $(h_{11/2})_\nu^{-1}\otimes 3^-$ component in the 3.04-MeV $(\frac{7}{2}^+)$ state. These observations, however, are merely qualitative indications for a more serious calculation of the energy levels of these nuclei.

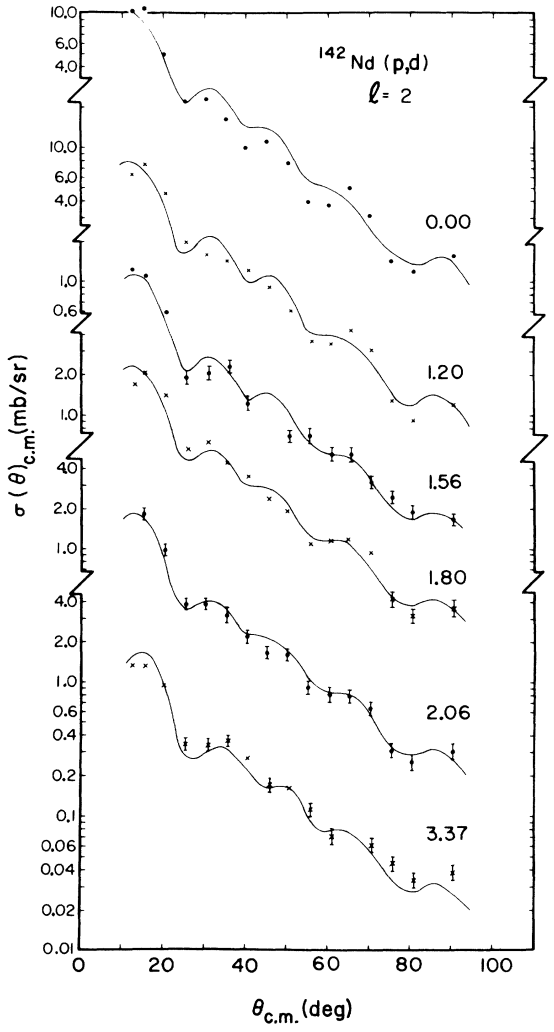

FIG. 12. A comparison of the experimental angular distributions for several states in ^{141}Nd (excitation energies on the right-hand side) with the NLFR-DWBA calculations for $l=2$. With the exception of the ground state, all others were assumed to have a spin and parity of $\frac{5}{2}^+$.

B. ^{142}Nd$(p,d)^{141}$Nd

A deuteron energy spectrum from this reaction measured at 70° is shown in the bottom part of Fig. 4. As in ^{144}Sm(p,d), the lowest four prominent peaks are the dominant components of $(2d_{3/2})_\nu^{-1}$, $(3s_{1/2})_\nu^{-1}$, $(1h_{11/2})_\nu^{-1}$, and $(2d_{5/2})_\nu^{-1}$ states in ^{141}Nd. Angular distributions of these and several other deuteron groups seen in Fig. 4 have been measured from 12.5 to 90° and compared with NLFR-DWBA calculations. The results of these comparisons are shown in Figs. 11–14.

Two $l=0$ groups at excitation energies of 0.19 and 1.87 MeV can be seen in Fig. 11. The broken curves going through the data points merely guide the eye. The DWBA cross sections only qualitatively agree with the experimental angular distributions.

Next, in Fig. 12 are six $l=2$ angular distributions, the shapes of which are reproduced quite well by the NLFR-DWBA calculations. For reasons given in the section on ^{144}Sm$(p,d)^{143}$Sm, only the ground state was assumed to have a spin and parity of $\frac{3}{2}^+$; all others were assigned $J^\pi=\frac{5}{2}^+$. An examination of the energy systematics of these $l=2$ states reveals that such a choice of spin and parity for the higher $l=2$ states is consistent with a similar choice in other $N=81$ nuclei.[25]

In Fig. 13, three $l=4$ angular distributions cor-

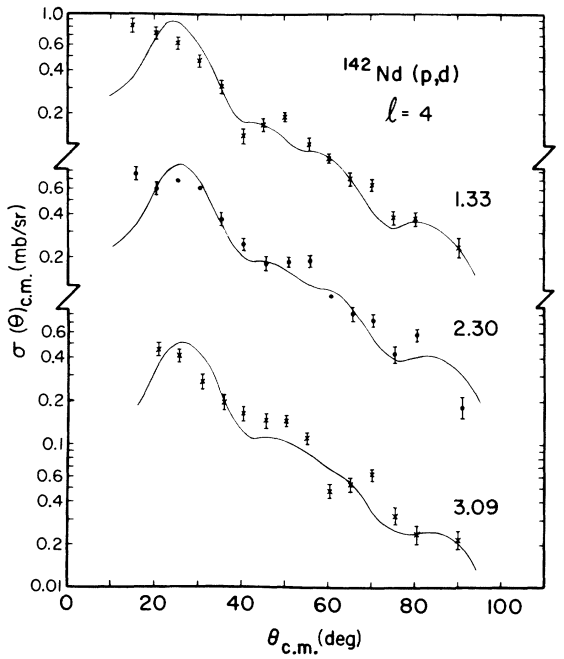

FIG. 13. A comparison of the experimental angular distributions for several states in ^{141}Nd (excitation energies shown on the right-hand side) with NLFR-DWBA calculations for $l=4$.

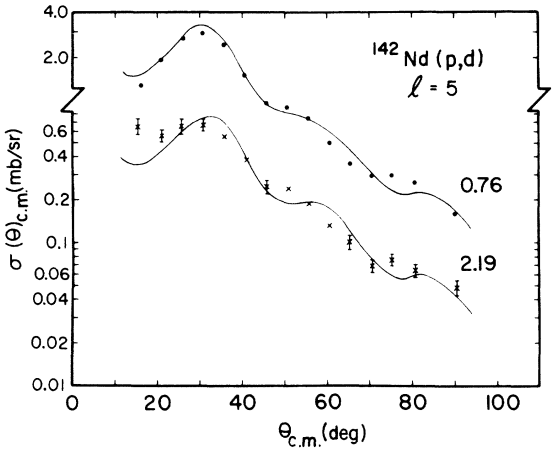

FIG. 14. A comparison of experimental angular distributions for three states in ^{141}Nd (excitation energies shown on the right-hand side) with NLFR-DWBA calculations for $l=5$.

responding to 1.33, 2.30, and 3.09 MeV of excitation energy in the residual nucleus can be seen. The very forward angle points in these angular distributions are probably high because of the large and difficult-to-determine background in most of the ^{142}Nd(p,d) spectra. Apart from the forward-angle points, the shapes of the experimental angular distributions are reproduced quite well by the NLFR-DWBA calculations.

In Fig. 14 two $l=5$ angular distributions are observed for groups corresponding to excitation energies of 0.76 and 2.19 MeV in ^{141}Nd. In the case of the 2.19-MeV group the data do not agree with the DWBA calculation for $l=4$ so that the present $l=5$ assignment is quite certain despite the poor agreement at the very forward angles. The energy of this $l=5$ group once again is consistent with the energies of analogous $l=5$ groups in the other $N=81$ nuclei studied in the present sequence.

The excitation energies of the various states observed in ^{142}Nd(p,d), their spins and parities, the absolute spectroscopic factors obtained by using Eq. (2), and the relative spectroscopic factors (i.e., when $S_{3/2}=4.0$) are listed in Table V. The uncertainty in the $\frac{5}{2}^+$ assignment for the weakly excited $l=2$ states merely reflects the fact that these assignments are based not on any J-dependent effects in the $l=2$ angular distributions but purely on

TABLE V. Excitation energies, l and J^π assignments, (p,d) cross sections at the observation angle θ, absolute and relative spectroscopic factors for the various states observed in the ^{142}Nd$(p,d)^{141}$Nd reactions.

Excitation energy (MeV)	l	J^π	$\theta_{c.m.}$ (deg.)	$\sigma(\theta)_{c.m.}$ (mb/sr)	S	S (relative)
0.00	2	$\frac{3}{2}^+$	25.3	2.30	4.1	4.0
0.19	0	$\frac{1}{2}^+$	20.2	4.10	1.9	1.9
0.76	5	$\frac{11}{2}^-$	25.3	2.70	9.0	8.7
1.20	2	$\frac{5}{2}^+$	25.3	2.00	3.3	3.3
1.33	(4)	$(\frac{7}{2}^+)$	20.2	0.72	3.6	3.5
1.56	2	$(\frac{5}{2}^+)$	35.4	0.23	0.5	0.5
1.80	2	$(\frac{5}{2}^+)$	40.4	0.35	1.2	1.1
1.87	0	$\frac{1}{2}^+$	25.3	0.24	0.34	0.32
2.06 {2.05 2.09	2	$(\frac{5}{2}^+)$	30.4	0.38	0.8	0.8
2.19	5	$\frac{11}{2}^-$	30.4	0.68	2.4	2.4
2.30 [a]	(4)	$(\frac{7}{2}^+)$	30.4	0.62	3.9	3.8
2.59	...	...	65.6	0.06	...	...
(2.80)	...	...	...	...	...	...
2.91	(2+4)	...	65.6	0.08	...	...
3.09	(4)	$(\frac{7}{2}^+)$	20.2	0.45	3.0	3.0
3.37	2	$(\frac{5}{2}^+)$	20.2	0.94	0.9	0.9
(3.49)	...	...	...	...	...	...
(3.58)	...	...	...	...	...	...
(3.89)	...	...	...	...	...	...

[a] Doublet (?).

arguments given in the section on ^{144}Sm(p, d).

The group at 2.06 MeV was resolved into a doublet with a position-sensitive detector ($\Delta E \sim 14$ keV) in the focal plane of our Enge split-pole spectrometer. This measurement was made at 20° and the relative intensity of the higher excitation energy group was observed to be only 20% of the total intensity. The angular distribution of the 2.06-MeV group in Fig. 12 agrees very well with the DWBA calculation for $l=2$ indicating that at least the lower-lying more intense group has $l=2$. Similarly the 2.30-MeV group seems to have at least two components ~25 keV apart. The line shape of the group, however, does not change with angle indicating that possibly both components of the group have the same angular distribution, i.e., $l=4$. This result is further supported by the fact that two close-lying $\frac{7}{2}^+$ states are observed in ^{143}Sm at approximately the same excitation energy. The spectroscopic factor of 3.8 is obtained for the combined strength. The groups within parentheses were observed in at least three different spectra at different angles but no angular distribution could be measured. Hence it is concluded that their existence needs further confirmation. The group corresponding to 2.91 MeV of excitation energy in ^{141}Nd has an angular distribution that can be fitted by an incoherent sum of $l=2$ and 4 DWBA cross sections so that it is quite likely that the 2.91-MeV state is also at least a doublet.

Figure 15 shows the energy levels of ^{141}Nd along with their spins, parities, and relative spectroscopic factors where these have been compared with the (d, t) results of Foster, Dietzsch, and Spalding[6] and the preliminary results of Bruge *et al.*[26]. The agreement in energies and spins and parities with the work of Foster, Dietzsch, and Spalding is very good as far as their measurements go. Their relative spectroscopic factors, although very similar to our spectroscopic factors, disagree in some cases by as much as 30%. There is probably a numerical error in their spectroscop-

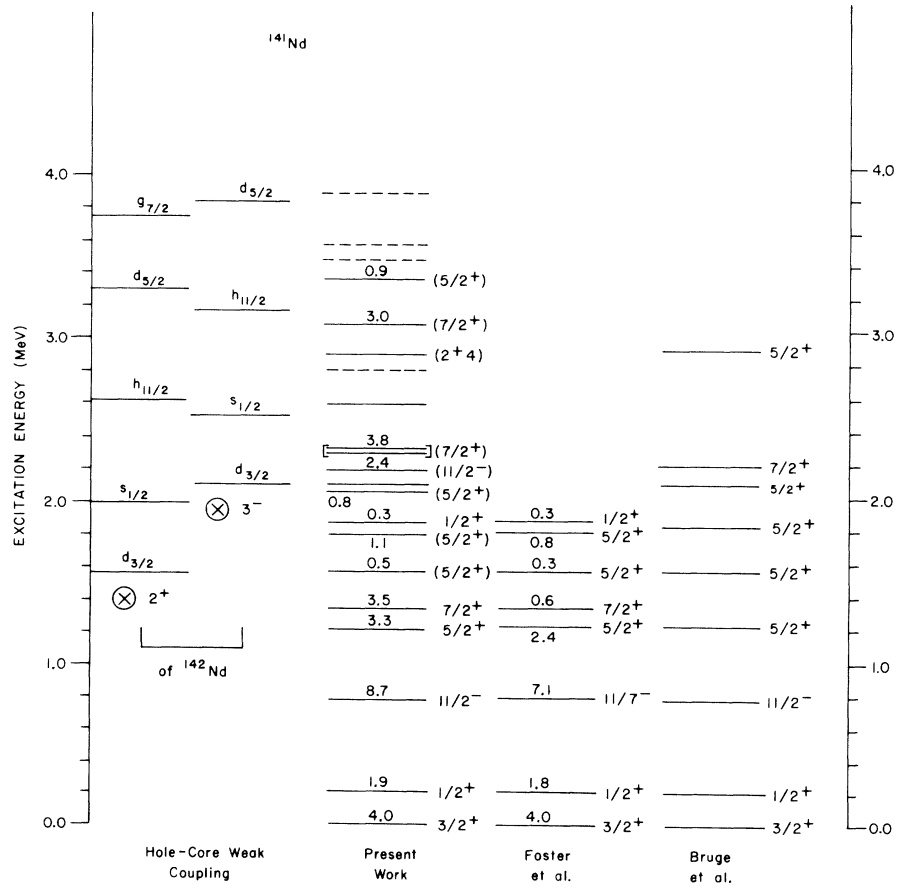

FIG. 15. A comparison of the present results in ^{142}Nd(p, d) with those of Foster *et al.* (Ref. 6) and Bruge *et al.* (Ref. 26). The numbers above the energy levels in the present work and that of Ref. 6 are relative spectroscopic factors. A comparison is also made between the neutron-hole states weakly coupled to the 2^+ and the 3^- core excitations of ^{142}Nd and the ^{141}Nd energy levels. See text for further comments.

ic factor for the 1.33-MeV $\frac{7}{2}^+$ state, as their number is about $\frac{1}{8}$th of our value. Our spectroscopic factor for this state, however, is consistent with that for an analogous (1.36-MeV) state in ^{143}Sm. In the case of the 2.19-MeV state, Bruge *et al.* assign it a $J^\pi = \frac{7}{2}^+$. Our angular distribution (Fig. 14) does not agree with the $l=4$ DWBA calculation at forward angles. Furthermore the energy systematics of the various components of the $(h_{11/2})_\nu^{-1}$ state[25] confirms our assignment of $\frac{11}{2}^-$. With regard to the 2.91-MeV state our data can be fitted with a suitable incoherent sum of $l=2$ and 4 DWBA cross sections as mentioned earlier. Hence we do not rule out the existence of a $\frac{5}{2}^+$ state at that energy.

The "centers of gravity" of the various neutron-hole-state components along with their summed hole strengths are listed in Table IV. The summed strengths are given in relative (i.e., $Sd_{3/2}=4.0$) and absolute values and have been compared with theoretical values derived from Eq. (4) where the proton occupation numbers for the shell-model orbits of interest were obtained from the (^{3}He, d) and (d,^{3}He) measurements of Wildenthal, Newman, and Auble.[28] With the exception of the $(1g_{7/2})_\nu^{-1}$ state the relative and absolute strengths are in good agreement (within the uncertainties of the present measurement) with the theoretical estimates. As pointed out earlier, the uncertainties in the $(1g_{7/2})_\nu^{-1}$ cross sections are large and consequently a somewhat larger difference (than is encountered for smaller l values) between the theoretical and the experimental spectroscopic strengths is not too surprising. In Fig. 15 the energy levels of ^{141}Nd have also been compared with the centers of gravity of states derived from the weak coupling of the neutron-hole states and the core-excited 2^+ and the 3^- states of ^{142}Nd. It appears that the 1.59-MeV d ($l=2$) state may have $2^+ \otimes (d_{3/2})_\nu^{-1}$ as an appreciable component of its wave function. A similar statement could perhaps also be made about the 3.37-MeV d state.

V. CONCLUSIONS

Some significant results of the present investigation are as follows:
(1) DWBA calculations including nonlocality corrections for both channels and also finite-range corrections for the effective p-n interaction, yield acceptable spectroscopic factors without any arbitrary normalization of the calculated cross sections. (2) Considerable splitting of the $(d_{5/2})_\nu^{-1}$ and $(g_{7/2})_\nu^{-1}$ states is observed. The $(d_{3/2})_\nu^{-1}$ state is presumably not fractionated. At least two components are observed for both the $(s_{1/2})_\nu^{-1}$ and the $(h_{11/2})_\nu^{-1}$ states, with the largest share of the total strength being in the lower-lying member. (3) No measurable population of any shell-model orbits in the $82 < N \leq 126$ major shell is observed indicating that the neutron shell closure at $N=82$ is a reasonably good assumption. (4) Several states that could be good candidates for a core-excitation –neutron-hole coupling model are identified.

ACKNOWLEDGMENTS

The authors sincerely appreciate the help of Dr. G. F. Trentelman in accumulating the data. Several very stimulating and helpful discussions with Dr. B. Preedom, Dr. B. H. Wildenthal, and Dr. J. Nolen are thankfully acknowledged.

---

†Work supported by the National Science Foundation.

[1]R. K. Jolly and C. F. Moore, Phys. Rev. 145, 918 (1966).
[2]D. Von Ehrenstein, G. C. Morrison, J. A. Nolen, Jr., and N. Williams, Phys. Rev. C 1, 2066 (1970).
[3]H. Christensen, B. Herskind, R. R. Borchers, and L. Westgaard, Nucl. Phys. A102, 481 (1967).
[4]K. Yagi, T. Ishimatsu, Y. Ishizaki, and Y. Saji, Nucl. Phys. A121, 161 (1968).
[5]R. H. Fulmer, A. L. McCarthy, and B. L. Cohen, Phys. Rev. 128, 1302 (1962).
[6]J. L. Foster, O. Dietzsch, and D. Spalding, to be published.
[7]D. B. Beery, W. H. Kelly, W. C. McHarris, Phys. Rev. 188, 1875 (1969).
[8]J. D. King, N. Neff, and H. W. Taylor, Nucl. Phys. A99, 433 (1967).
[9]D. DeFrenne, J. Demuynck, H. Heyde, E. Jackobs, M. Dorikens, and L. Dorikens-Vanpraet, Nucl. Phys. A106, 350 (1968).
[10]D. Bayer, Ph.D. thesis, Michigan State University, 1970 (unpublished).
[11]Nuclear reaction Q values: C. Maples, G. W. Goth, and J. Cerny, University of California Radiation Laboratory Report No. UCRL-16964, 1966 (unpublished).
[12]R. K. Jolly, G. F. Trentelman, and E. Kashy, Nucl. Instr. Methods 87, 325 (1970).
[13]R. H. Bassel, R. M. Drisko, and G. R. Satchler, Oak Ridge National Laboratory Report No. 3240, 1962 (unpublished); and a subsequent Oak Ridge National Laboratory memorandum to users of JULIE, 1966 (unpublished).
[14]F. G. Perey, Phys. Rev. 131, 745 (1963).
[15]M. P. Fricke, E. E. Gross, B. J. Morton, and A. Zucker, Phys. Rev. 156, 1207 (1967).
[16]C. M. Perey and F. G. Perey, Phys. Rev. 132, 755 (1963).
[17]F. G. Perey and D. S. Saxon, Phys. Letters 10, 107 (1964).
[18]F. G. Perey, in *Proceedings of the Rutherford Jubilee International Conference, Manchester, England, 1961,*

edited by J. B. Birks (Heywood and Company, Ltd., London, 1962), p. 125.
[19]A. M. Green, Phys. Letters 24B, 382 (1967).
[20]B. M. Preedom, J. L. Snelgrove, and E. Kashy, Phys. Rev. C 1, 1132 (1970).
[21]R. M. Drisko, private communication.
[22]J. B. French and M. H. Macfarlane, Nucl. Phys. 26, 168 (1961).
[23]W. C. Parkinson, D. L. Hendrie, H. H. Duhm, J. Mahoney, J. Saudinos, and G. R. Satchler, Phys. Rev. 178, 1976 (1969).
[24]S. Hinds, R. Middleton, J. H. Bjerregaard, O. Hanson, and O. Nathan, Nucl. Phys. 83, 17 (1966).
[25]R. K. Jolly and E. Kashy, to be published.
[26]G. Bruge, A. Chaumeaux, Ha Duc Long, and J. Picard, Centre d'Études Nucléaires de Saclay Progress Report, October, 1968–September, 1969 (unpublished).
[27]V. R. W. Edwards, N. K. Ganguly, D. G. Montague, K. Ramavataram, A. Zucker, and D. J. Plummer, Rutherford High-Energy Laboratory Program Report No. RHEL/R187, 1967 (unpublished).
[28]B. H. Wildenthal, E. Newman, and R. L. Auble, Phys. Rev. C 3, 1199 (1971).

PHYSICAL REVIEW C VOLUME 4, NUMBER 3 SEPTEMBER 1971

Distribution of Partial Radiation Widths in $^{238}U(n,\gamma)^{239}U$†

O. A. Wasson and R. E. Chrien
Brookhaven National Laboratory, Upton, New York 11973
and
G. G. Slaughter and J. A. Harvey
Oak Ridge National Laboratory, Oak Ridge, Tennessee 37830
(Received 22 March 1971)

The resonant-neutron-capture γ-ray spectra for 28 resonances below 600-eV neutron energy are measured in $^{238}U(n,\gamma)^{239}U$ with improved neutron and γ-ray energy resolution to allow an accurate test of the predictions of the statistical model of neutron capture. No convincing departures from these predictions are observed. The variation over 23 S-wave neutron resonances of the γ-ray transition probabilities to 15 final states is consistent with the Porter-Thomas distribution for both $E1$ and $M1$ multipoles. There is also no statistically significant correlation between the different decay modes of the neutron resonances. A large correlation coefficient of +0.81 is observed between the partial radiative widths of the 3991- and 3982-keV γ rays. This result, however, is not in violation of statistical independence for a sample size of 15 γ rays. The $E1$ and $M1$ γ-ray strength functions are $(2.6\pm0.4)\times10^{-3}$ and $(8.1\pm1.6)\times10^{-3}$, respectively, compared to 3×10^{-3} and 4×10^{-3} listed by Bartholomew as the median values of all nuclei. Three of the weaker resonances at 10.2, 89.5, and 263 eV are assigned to P-wave capture. The neutron binding energy is measured to be 4806.7±2.0 keV, which is 5.0 keV higher than the previously accepted value. Previously unobserved γ-ray transitions are reported.

I. INTRODUCTION

Two of the predictions of the statistical model of nuclear reactions are that the various decay modes of the resonant states formed in neutron capture should be independent, and that the radiative transition widths for γ-ray decay from these highly excited nuclear states should fluctuate widely from capturing state to capturing state and also be independent of specific nuclear structure properties. In particular, the distribution over neutron resonances of γ-ray transitions to a particular final state should follow a χ^2 distribution with one degree of freedom, the so-called Porter-Thomas distribution.[1] Many of the nuclides studied in the resonant (n,γ) reaction are found to be consistent with this last prediction.

However, apparent departures from the Porter-Thomas distribution are reported[2-5] for resonant neutron capture in the target nuclei ^{238}U, ^{103}Rh, ^{141}Pr, and ^{175}Lu. In addition, significant correlations between different decay modes of the nuclear states above the neutron binding energy and observed. Correlations between the reduced neutron widths of the resonances and the γ-ray transition probabilities to a particular final nuclear state are observed[6-8] for resonant neutron capture in the target nuclei ^{170}Tm and ^{163}Dy. A similar correlation was observed[9] in the inverse reaction $^{207}Pb(\gamma,n)^{206}Pb$. These correlations are interpreted as resulting from the contribution of particle-hole or "doorway states" to the resonant levels[10,11] and indicate departures from the statistical concept of the compound nucleus.